


Article

# Inclusion Complex between Local Anesthetic/2-hydroxypropyl- $\beta$ -cyclodextrin in Stealth Liposome

Gredson Keiff Souza <sup>1</sup>, André Gallo <sup>2</sup>, Luiza Hauser Novicki <sup>2</sup>, Heitor Rodrigues Neto <sup>2</sup>, Eneida de Paula <sup>3</sup> , Anita Jocelyne Marsaioli <sup>1</sup> and Luis Fernando Cabeça <sup>2,\*</sup>

<sup>1</sup> Chemistry Institute, State University of Campinas, UNICAMP, Rua Josué de Castro Cidade Universitária, Campinas CEP 13083-970, Brazil; gredsonkeiff@hotmail.com (G.K.S.); anita@iqm.unicamp.br (A.J.M.)

<sup>2</sup> Chemistry Department, Technological Federal University of Parana, UTFPR, Avenida dos Pioneiros, Londrina CEP 86036-370, Brazil; andre28gallo@gmail.com (A.G.); luizanovicki@alunos.utfpr.edu.br (L.H.N.); heitor\_rneto@hotmail.com (H.R.N.)

<sup>3</sup> Biology Institute, State University of Campinas, UNICAMP, Rua Josué de Castro Cidade Universitária, Campinas CEP 13083-970, Brazil; depaula@unicamp.br

\* Correspondence: luiscabeça@utfpr.edu.br; Tel.: +55-43-98040615

**Abstract:** The drugs delivery system in the treatment of diseases has advantages such as reduced toxicity, increased availability of the drug, etc. Therefore, studies of the supramolecular interactions between local anesthetics (LAs) butamben (BTB) or ropivacaine (RVC) complexed with 2-hydroxypropyl- $\beta$ -cyclodextrin (HP- $\beta$ CD) and carried in Stealth liposomal (SL) are performed. <sup>1</sup>H-NMR nuclear magnetic resonance (DOSY and STD) were used as the main tools. The displacements observed in the <sup>1</sup>H-NMR presented the complexation between LAs and HP- $\beta$ CD. The diffusion coefficients of free BTB and RVC were  $7.70 \times 10^{-10} \text{ m}^2 \text{ s}^{-1}$  and  $4.07 \times 10^{-10} \text{ m}^2 \text{ s}^{-1}$ , and in the complex with HP- $\beta$ CD were  $1.90 \times 10^{-10} \text{ m}^2 \text{ s}^{-1}$  and  $3.64 \times 10^{-10} \text{ m}^2 \text{ s}^{-1}$ , respectively, which indicate a strong interaction between the BTB molecule and HP- $\beta$ CD (98.3% molar fraction and  $K_a = 72.279 \text{ L/mol}$ ). With STD-NMR, the encapsulation of the BTB/HP- $\beta$ CD and RVC/HP- $\beta$ CD in SL vesicles was proven. Beyond the saturation transfer to the LAs, there is the magnetization transfer to the hydrogens of HP- $\beta$ CD. BTB and RVC have already been studied in normal liposome systems; however, little is known of their behavior in SL.

**Keywords:** butamben; ropivacaine; stealth liposomes; <sup>1</sup>H-NMR; NMR-STD



**Citation:** Souza, G.K.; Gallo, A.; Novicki, L.H.; Neto, H.R.; de Paula, E.; Marsaioli, A.J.; Cabeça, L.F. Inclusion Complex between Local Anesthetic/2-hydroxypropyl- $\beta$ -cyclodextrin in Stealth Liposome. *Molecules* **2022**, *27*, 4170. <https://doi.org/10.3390/molecules27134170>

Academic Editor: Silvia Arpicco

Received: 1 June 2022

Accepted: 20 June 2022

Published: 29 June 2022

**Publisher's Note:** MDPI stays neutral with regard to jurisdictional claims in published maps and institutional affiliations.



**Copyright:** © 2022 by the authors. Licensee MDPI, Basel, Switzerland. This article is an open access article distributed under the terms and conditions of the Creative Commons Attribution (CC BY) license (<https://creativecommons.org/licenses/by/4.0/>).

## 1. Introduction

Nuclear magnetic resonance (NMR) is one of the most important spectroscopic techniques for the investigation of supramolecular systems with interdisciplinary applications. NMR may promote evidence on the formation and topology of inclusion complexes formed by multiple components resulting from non-covalent hydrophobic interactions. The study of the different techniques based on <sup>1</sup>H-NMR can promote evidence of a molecular self-assembly process, as well as the formation of a host-guest complex [1–3]. Such evidence is extracted from changes in chemical displacement, Overhauser nuclear effect, relaxation, and diffusion coefficient measurements. In this context, <sup>1</sup>H-NMR methods were developed and applied in the screening and characterization of supramolecular complexes such as: rotational nuclear Overhauser effect spectroscopy (ROESY 1D) [4] diffusion-ordered spectroscopy (DOSY) [5] and saturation transfer difference (STD) [6].

Host molecules such as cyclodextrins (CDs) present in their structure a ring shape with a hydrophilic outer part, which ensures excellent aqueous solubility, and an internal apolar cavity, which can accommodate guest molecules. CDs allow the formation of stable inclusion complexes with a great diversity of organic substances [7,8]. CDs are composed of a group of pharmaceutical excipients composed of units of D-glucopyranose (cyclic sugars), of six, seven, and eight, called  $\alpha$ -cyclodextrin ( $\alpha$ CD),  $\beta$ -cyclodextrin ( $\beta$ CD) and

$\gamma$ -cyclodextrin ( $\gamma$ CD).  $\beta$ -cyclodextrin is the most used, due to its favorable cavity size for medications [8,9]. It is noteworthy that cyclodextrins are not considered controlled drug release systems because they release the assets quickly as soon as they enter the bloodstream [9]. However, they are widely used to improve the solubility of insoluble compounds [7].

The carriers with excellent characteristics for controlled release are the liposome vesicles and they work as carriers (transporters) of drugs and biomolecules, regardless of their load or molar mass [9,10]. Usually, the liposomes are composed of phospholipids, that form stable concentric bilayers in an aqueous solution. Phosphatidylcholines present great stability in the face of pH or salt concentration variations in the medium [10,11].

The liposomes may also present modified membranes with polyethylene glycol originating long-lasting liposomes or stealth liposomes (SL). SL has a longer half-life time since it avoids the recognition and capture of these by the mononuclear phagocytic system due to the increase in vesicles solvation [12]. The use of SL, in addition to increasing circulation time, also promotes an improvement in the stability of the complex and of the drug (by inhibiting degradation by enzymes and by reducing renal clearance of small molecules) [12] and decreased liposomal vesicle disintegration [13]. This is mainly because Poly(ethylene glycol) (PEG) is non-ionic, has low fouling, and has a high solubility in aqueous and organic media, which allows for the synthesis of PEGylated lipids, as well as facilitating the formulation of stealthy liposomes, which requires the solubilization of the PEG-lipopolymer [14].

Studies in the literature show that double drug encapsulation in cyclodextrins in liposomes can bring advantages such as better solubility of hydrophobic actives, inclusion complexes with controlled release properties, stability, and improvement to the integrity of its structure, reduction in toxicity and prolongation of drug time after being administered orally or parenterally [11,15,16].

An example of drugs encapsulated in liposomes that have been widely studied in the literature is local anesthetics (LA). Complexes formed with LA/liposomes show the advantages of the slow release of the drug, which prolongs the duration of anesthesia and reduction in toxicity to the cardiovascular and central nervous systems [11,17]. Great advances have been made in research involving liposomes and local anesthetics, which are promising in relation to the use of the free drug [18–20].

Ternary systems involving the anesthetic ropivacaine (RVC), HP- $\beta$ CD, and liposomes were studied by Vieira et al. [11]. They observed that the anesthetic effect in the ternary system was able to prolong the RVC effect and the release of kinetics was also observed in cytotoxicity tests, thus reflecting a stronger interaction of RVC and HP- $\beta$ CD. Moreover, local anesthetics such as ropivacaine and butamben (RVC, BTB) encapsulated in ternary systems open the prospect of promoting the potential long-term anesthesia with reduced cytotoxicity. However, it is of fundamental importance to have precise knowledge of the interaction between the compounds involved in the system, as well as the topology of the formed complex. Knowledge of this type of interaction can provide support for the development of more effective and potent anesthetics.

Hence, the present work focuses on developing a formulation for local anesthetic butamben (BTB) and ropivacaine (RVC) in a binary system, through its complexation in 2-hydroxypropyl- $\beta$ -cyclodextrin (HP- $\beta$ CD), followed by encapsulation in stealth liposomes. The study of the supramolecular interaction of different complexes was performed by nuclear magnetic resonance through spectroscopic analysis of  $^1\text{H-NMR}$ , DOSY and  $^1\text{H-STD}$ .

## 2. Results and Discussion

### 2.1. Subsection Complexing Efficiency (EE) and Constant Association (Ka) for BTB and RVC in HP- $\beta$ CD

One of the objectives was to determine the encapsulation efficiency (EE) and affinity constant (Ka) of the complexes. UV-vis spectrophotometry was used for the anesthetic BTB and RVC.

For the EE and Ka calculations of local anesthetics RVC and BTB in HP- $\beta$ CD, an anesthetic calibration curve was first performed. For the LA BTB, we presented the equation of equal line (Equation (1)) [7] and standard solubility data of BTB ( $S_0$ ) in buffer solution pH 7.4,  $S_0 = 0.66 \times 10^{-3}$  M for free BTB. Mura et al. [21] found the solubility of 0.86 mM.

$$Y(\text{abs}) = -0.0039 + 24.907 \times [\text{BTB}] \quad (R^2 = 0.99884) \quad (1)$$

As absorbance is an inherent property of each substance, in which different materials can absorb radiation at different wavelengths, absorption spectra were obtained in the UV region for both the determination of  $S_0$  and for the analytical curve of BTB (282 nm).

The absorbance values obtained from BTB at different concentrations of HP- $\beta$ CD were used to find the value of the encapsulated BTB concentration, with the aid of the equation of the line of the calibration curve (Equation (1)) [22], as shown in Figure 1A.

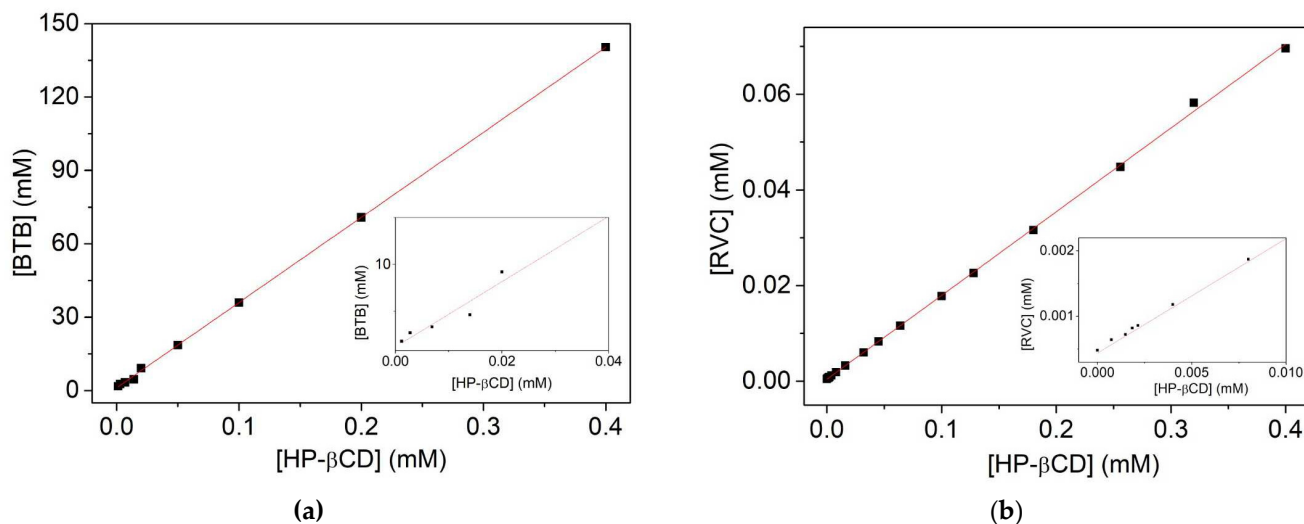


**Figure 1.** (a) BTB Solubility in HP- $\beta$ CD (slope = 0.3479,  $R^2 = 0.99977$ ); (b) RVC Solubility Graphic In HP- $\beta$ CD (slope = 0.175,  $R^2 = 0.9994$ ). Determined at room temperature ( $n = 3$ ).

The soluble phase of BTB in HP- $\beta$ CD solution at pH 7.4 provided the equation of the line (Equation (2)). As shown in Figure 1A, it is noted that there is a formation of the binary complex of BTB and cyclodextrin, since the solubility diagram demonstrates that the drug has become more soluble as the concentration of HP- $\beta$ CD increases [23]. The encapsulation efficiency (EE) of BTB in HP- $\beta$ CD was 0.534, and it was calculated using the slope/1-slope equation (Equation (5)) [24,25]. According to Barbosa et al. [26] the higher the encapsulation efficiency, the lower the amount of cyclodextrin required for the solubilization of the drug, therefore, the closer it is to 1, and better the EE. Mura et al. [21] observed that the solubility of BTB increased linearly with the increase in the concentration of CDs, with the formation of highly soluble complexes in stoichiometry (1:1).

$$[\text{BTB}] = 0.34797 \times [\text{HP-}\beta\text{CD}] + 1.19876 \quad (R^2 = 0.9997). \quad (2)$$

The increase in the aqueous solubility of BTB in HP- $\beta$ CD was used as a measure of complex formation. The value of the determined association constant (Ka) was  $K_a = 808 \text{ M}^{-1}$  at pH 7.4 (where the  $S_0$  used was  $0.66 \times 10^{-3}$  M) Figure 1a. The value of the association constant (Ka) is used to compare the affinity of the drug with HP- $\beta$ CD

and also to classify the extent of chemical-physical changes that occurred after complexation. These values can range between  $10 \text{ M}^{-1}$  and  $1000 \text{ M}^{-1}$ , and this unit is valid only for complexes with 1:1 stoichiometry [27]. In addition, Moraes et al. [28] point out that local amino-ester anesthetics present higher formation constant values, such as  $K_a = 549 \text{ M}^{-1}$  for benzocaine and  $K_a = 351 \text{ M}^{-1}$  for tetracaine. Thus, these results are in agreement with the literature. Maestrelli et al. [28] reported constant values of solubility of the order of  $273 \text{ M}^{-1}$  at pH 5. Moreover, this value depends both on the drug used and the medium in which it forms the complex with the carrier molecule. The value of the binding constant ( $K_a$ ) is used to compare the affinity of the drug with HP- $\beta$ CD.

The increase in total solubility of BTB in HP- $\beta$ CD was  $0.80 \times 10^{-3} \text{ M}$ , (about 21%); therefore, the solubility of the drug has a small increase in relation to the free BTB in an aqueous solution with pH 7.4. This result can be explained taking into account the use of low HP- $\beta$ CD. High HP- $\beta$ CD concentration values exhibit high values of encapsulated BTB absorption and eventually exceed detection limits [25]. In addition, the drug BTB already presents a good solubility even in the absence of the carrier molecule. Maestrelli et al. [28] reported BTB doubly loaded as a complex in liposome and hydroxypropyl-cyclodextrin; consequently, the complex showed good solubility and dissolution properties. The ratio BTB:HP- $\beta$ CD was 1:4, which demonstrates that to form a 1:1 complex (HP- $\beta$ CD:BTB) it is necessary four molecules of HP- $\beta$ CD and a molecule of BTB in the solution [22,28].

For the EE and  $K_a$  calculations of the HP- $\beta$ CD:RVC complex, a calibration curve of the RVC drugs ( $\lambda = 263 \text{ nm}$ ) was first performed. For the RVC, we had the equation of the same line (Equation (3)) [7], where Y is the concentration of RVC and Abs absorption ( $R^2 = 0.99945$ ).

$$Y_{[\text{RVC}]} = -3.3586 \times 10^{-4} + 0.0025 \text{ abs} \quad (3)$$

The absorbance values obtained from RVC at different concentrations of HP- $\beta$ CD were used to find the value of the encapsulated RVC concentration, with the aid of the equation of the line of the calibration curve, as shown in Figure 1B.

The soluble phase of RVC in aqueous HP- $\beta$ CD solution (Figure 1b) provided the equation of the line (Equation (4)) ( $R^2 = 0.99942$ ) [7]. The encapsulation efficiency (EE) of the RVC in HP- $\beta$ CD was 0.210, and the value of the determined association constant ( $K_a$ ) was  $441 \text{ M}^{-1}$  at pH 7.4 ( $K_d$  of 0.002 M), being  $S_0 = 0.00048 \text{ M}$ . The total solubility ( $S_t$ ) of RVC in the presence of HP- $\beta$ CD was 85 mM, 177 times higher than RVC in aqueous pH 7.4 solution. The RVC:HP- $\beta$ CD ratio was 1:6. This result shows that in a 1:1 complex (RVC:HP- $\beta$ CD) only one HP- $\beta$ CD molecule in every six RVC molecules is forming the inclusion complex with RVC. However, for other local anesthetics, similarities in molar ratio were observed [11,23,29].

$$[\text{RVC}] = 0.1750 \times [\text{HP-}\beta\text{CD}] + 0.00044 \quad (4)$$

## 2.2. Analysis of LA/HP- $\beta$ CD, LA/SL and LA/HP- $\beta$ CD/SL Complexes Using Nuclear Magnetic Resonance (LA = BTB and RVC)

The characterization of the complexes was also performed by the spectroscopic technique of  $^1\text{H-NMR}$ . The first piece of evidence for the formation of a complex can be observed by varying the chemical shift in the  $^1\text{H-NMR}$  spectrum [1]. Figure 2 and Table 1 show the structures of the molecules of RVC, BTB, HP- $\beta$ CD and the chemical shift of hydrogens, respectively.

For the RVC/SL complex, the highest values of shift variation were in ( $\Delta\delta = 0.22$ ) (H12; H11a);  $\Delta\delta = 0.89$  (H14). These values of chemical shift variation indicate that the cyclohexane ring of RVC is interacting with SL with greater intensity than the aromatic part of the molecule. The RVC/HP- $\beta$ CD complex has little shift variation. For the RVC/HP- $\beta$ CD/SL complex, there is also a low variation in the  $^1\text{H}$  RVC chemical shift, except for H12, H11a.

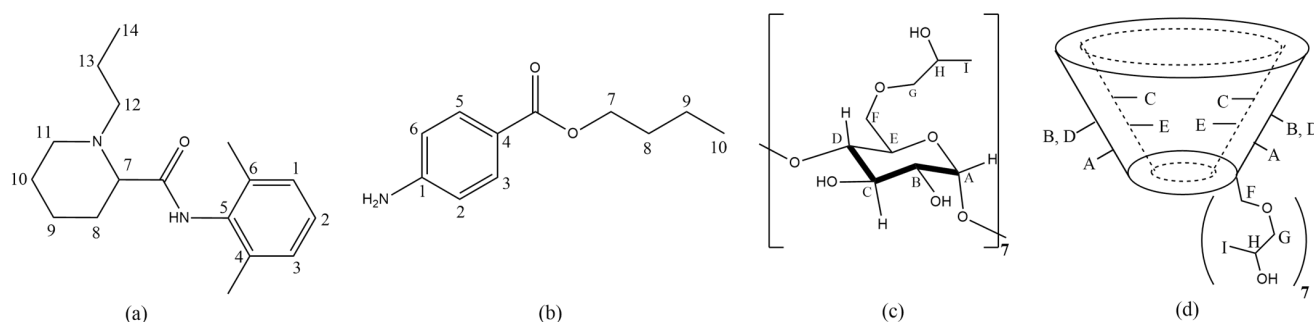


**Figure 2.** Structures of the molecules of (a) RVC; (b) BTB; (c,d) HP- $\beta$ CD.

**Table 1.** Attribution and chemical shift of BTB  $^1\text{H}$  and RVC  $^1\text{H}$  in the binary and ternary complexes.

H	BTB (ppm)	BTB/SL $\delta$ $^1\text{H}$ (ppm)	$\Delta\delta$ (ppm)	BTB/HP- $\beta$ CD (ppm)	$\Delta\delta$ (ppm)	BTB/HP- $\beta$ CD/SL (ppm)	$\Delta\delta$ (ppm)
2	6.76	-	-	6.69	-0.07	6.67	-0.02
3	7.78	-	-	7.66	-0.12	7.66	0.00
5	7.78	-	-	7.66	-0.12	7.66	0.00
6	6.76	-	-	6.69	-0.07	6.67	-0.02
7	4.23	-	-	4.26	0.03	-	-
8	1.66	-	-	1.68	0.02	1.68	0.00
9	1.36	-	-	1.39	0.03	1.38	0.01
10	0.87	-	-	0.91	0.04	0.92	0.01
H	RVC * (ppm)	RVC/SL * $\delta$ $^1\text{H}$ (ppm)	$\Delta\delta$ (ppm)	RVC/HP- $\beta$ CD * (ppm)	$\Delta\delta$ (ppm)	RVC/HP- $\beta$ CD/SL * (ppm)	$\Delta\delta$ (ppm)
1,2,3 Aromatic	7.14	7.14	0.00	7.15	0.01	7.14	-
7	4.12	4.10	-0.02	4.10	-0.02	-	-
8 <sub>e</sub>	2.37	2.37	0.00	2.37	0	-	-
11 <sub>e</sub>	3.67	-	-	-	-	-	-
12, 11 <sub>a</sub>	3.08	3.30	0.22	3.06	-0.02	3.17	0.09
15, 16	2.12	2.12	0.00	2.14	0.02	2.14	0.02
14	0.89	0.89	0.89	0.9	-0.01	0.90	0.01

<sub>a</sub> axial hydrogen; <sub>e</sub> equatorial hydrogen; \* concentration = 10 mM

A small variation in the chemical shift of BTB in the inclusion complexes can be seen in Table 1. Variations of  $-0.12$  for H3 and H5 in the BTB/HP- $\beta$ CD and of  $-0.02$  for H2 and H6 complex for BTB/HP- $\beta$ CD/SL complex is also present. To prove the formation of the BTB/HP- $\beta$ CD/SL complex encapsulation, efficiency tests of BTB were performed. EE values were found from 81.1% for the BTB/SL complex, and 84.2% for BTB/HP- $\beta$ CD/SL; these values show that BTB is mostly encapsulated. According to the literature [29,30], the aromatic ring is expected in the cavity of the carrier, and interactions of the aromatic rings of BTB and RVC in the cavity of HP- $\beta$ CD were observed.

Information regarding the variation in internal hydrogens of the HP- $\beta$ CD cavity is important. This can happen due to the presence of molecules inside the cavity. An example is the  $^1\text{H}$  chemical shift variation in HC in the BTB/HP- $\beta$ CD complex.

Another variation in HP- $\beta$ CD hydrogens was in HA and HF. The hydrogens HA and HF (hydrogens near the lower cavity of HP- $\beta$ CD) showed varying values in the chemical displacement of  $-0.03$  and  $-0.06$  ppm, respectively. This fact is due to the hydrogen bonds between the amino group or ester from BTB, with the HP- $\beta$ CD hydroxide group. For the RVC/HP- $\beta$ CD complex, the variation in the chemical shift of HP- $\beta$ CD also was small. A possible topology for the inclusion of LA in HP- $\beta$ CD was suggested in Figure 3.

For a better compression of binary and ternary inclusion complexes,  $^1\text{H}$  spectra of DOSY NMR were performed. From the diffusion coefficient data, the molar fraction (fx) and the association constant ( $K_a$ ) of the complexes were calculated, as shown in Table 2.



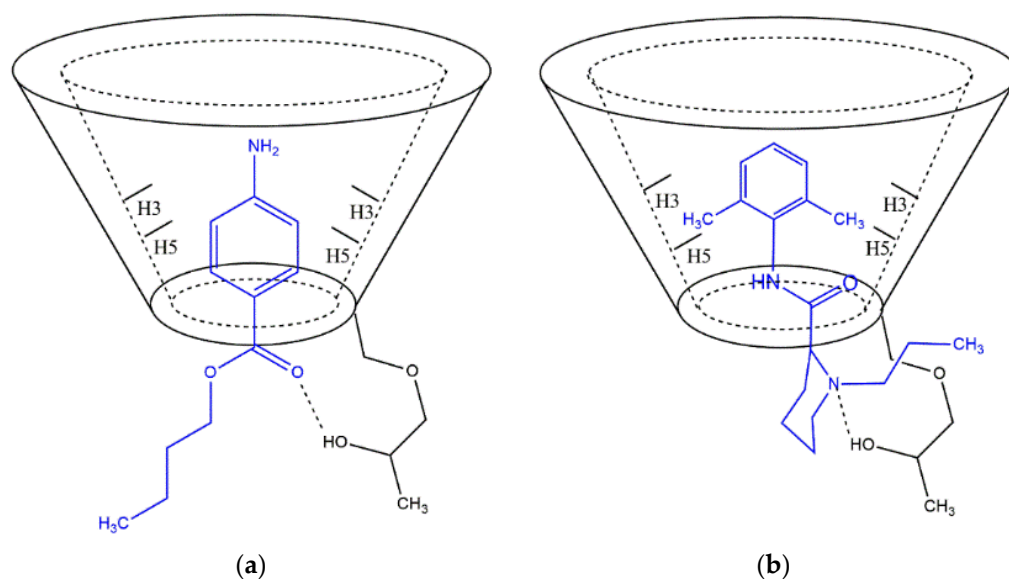


**Figure 3.** (a) Alternative topology for the BTB/HP- $\beta$ CD and (b) RVC/HP- $\beta$ CD complex.

**Table 2.** Diffusion coefficients ( $D$ ) of LA (BTB, RVC), HP- $\beta$ CD and LA/HP- $\beta$ CD, LA/HP- $\beta$ CD/SL constant association ( $K_a$ ) and molar fraction ( $f_x$ ).

Complex	Compounds	$D$ ( $10 \times -10 \text{ m}^2 \text{ s}^{-1}$ )	Molar Fraction of $f_x$ % Complex	$K_a$ L/mol
RVC/SL RVC/HP- $\beta$ CD RVC/HP- $\beta$ CD/SL	RVC	$4.07 \pm 0.40$		
	SL	$0.32 \pm 0.17$		
	HP- $\beta$ CD	$2.04 \pm 0.03$		
		$3.38 \pm 0.05$	18	28
		$3.64 \pm 0.02$	22	37
		$3.14 \pm 0.12$	25	44
BTB/HP- $\beta$ CD	BTB	$7.70 \pm 0.12$	98.3	72,279

RVC—Ropivacaine; BTB—Butamben; SL—Stealth liposomes; D—Diffusion Coefficients; HP- $\beta$ CD—2-Hydroxypropyl- $\beta$ -cyclodextrin.

For the RCV/SL complex, a molar fraction value of the 18% complex is found with its constant association  $28 \text{ L mol}^{-1}$ , which proves the association of RVC and SL. The formation of inclusion complex in a solution containing a drug and cyclodextrin can be observed by reducing its diffusion coefficient ( $D$ ). The greater the difference between  $D$  in solution with cyclodextrin compared to the  $D$  obtained from the solution without cyclodextrin, the greater the fraction of the drug inclusion complex [31].

The RVC/HP- $\beta$ CD and RVC/HP- $\beta$ CD/SL complexes indicated a complex fraction value of 22% and 24%, respectively; thus, approximately 25% of the RVC is complex. For the constant association, there is 37 and 44 L/mol of the RVC/HP- $\beta$ CD and RVC/HP- $\beta$ CD/SL complex, respectively. According to Araujo et al. [24] the typical chemical structure of LAs is characterized by a hydrophilic region (an amine group) and another hydrophobic region (usually an aromatic ring) separated by a polar group of the ester or amide type, which can generate differences in the proportion between the neutral and the charged form that is responsible for the speed of action. These characteristics present relatively low  $pK_a$  values, between 7.6–8.9.

For the BTB/HP- $\beta$ CD complex, the high molar fraction value of the obtained complex was 98.3%, jointly with its high constant association ( $72.279 \times 10^3 \text{ L mol}^{-1}$ ), which proves the association of BTB and the HP- $\beta$ CD molecule. The results corroborate the high values found for  $K_a$  for the UV-vis experiment ( $K_a 808 \text{ M}^{-1}$ ). Values of the BTB/SL and BTB/HP- $\beta$ CD/SL complex were not reported because no BTB signals were not obtained in the

complex spectrum. This is probably due to the fact that BTB is not in equilibrium between the aqueous phase and SL.

For better observation of the inclusion complexes between liposomes and the local anesthesia BTB or RVC, experiments of  $^1\text{H}$  NMR of saturation transfer differ (STD) were applied to study the local anesthetic-liposome interactions [32,33].

The STD experiment provides information on the hydrogens of the molecule BTB or RVC and HP- $\beta$ CD that are encapsulated in the SL vesicle. Figure 4 indicates the STD spectrum for the BTB/HP- $\beta$ CD/SL complex. Figure 4A refers to the  $^1\text{H}$  spectrum of the ternary complex. Figure 4B expresses the control spectrum (out of resonance) and Figure 4C the STD spectrum. In the region of 3 to 4 ppm, very intense signals were observed. They refer to the hydrogens of polyethylene glycol (PEG) and HP- $\beta$ CD, which are overlapping; therefore, this region was discarded for STD analysis.

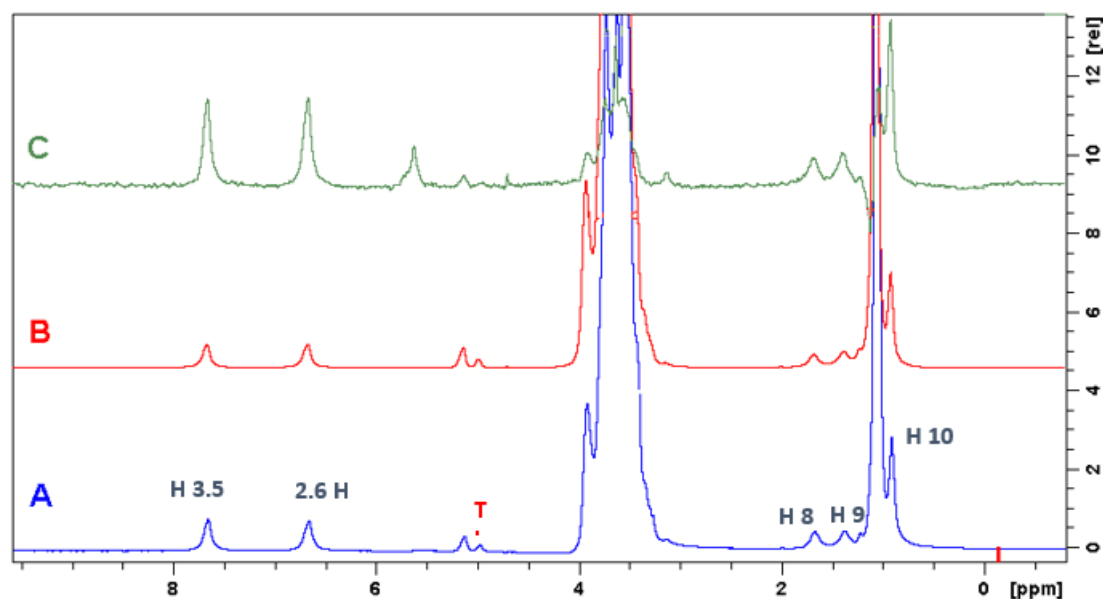


**Figure 4.** (A)  $^1\text{H}$  NMR spectrum (400 MHz,  $\text{D}_2\text{O}$ /residual  $\text{H}_2\text{O}$  reference at 4.7 ppm) of the BTB/HP- $\beta$ CD/SL complex ( $50 \text{ mmol L}^{-1}$ ); (B) control spectrum (radiating at 30 ppm); (C) STD spectrum (radiating at  $-0.5$  ppm). Total saturation time 2.55 s.

The STD spectrum (irradiated at  $-0.5$  ppm) indicated that the liposome saturation transfer to BTB and HP- $\beta$ CD hydrogens occurred; this indicates that both molecules were encapsulated in SL [32,33]. For the hydrogens signals of HP- $\beta$ CD, it was not possible to calculate the transference of the magnetization percentage due to the overlap of the signals. For the BTB molecule, the aromatic hydrogens H2, H3, H5, and H6 presented the highest magnetization transfer rates (97%), followed by H8 (87.5%) as shown in Table 3.

**Table 3.** Data obtained in the STD experiments.

Frequency (ppm)	Area STD	Area Outside Resonance	Map STD Standardized
H2 e 6 BTB = 6.67	0.0242	0.8989	97.4%
H3 e 5 BTB = 7.66	0.0234	0.8575	97.3%
H9 BTB = 1.38	0.1550	1.0000	84.6%
H8 BTB = 1.68	0.1639	1.3054	87.5%
H14 RVC = 0.90	0.0035	1.3873	34%
H1, H2, H3 RVC = 7.14	0.0074	1.0000	100%
H15, H16 RVC = 2.14	0.0049	1.8851	35%

The STD experiment also provided an analysis of the ternary complex RVC/HP- $\beta$ CD/SL. This analysis provides information about the hydrogens of the RVC molecule

and the HP- $\beta$ CD that are encapsulated in the SL vesicle (Figure 5). Figure 5C refers to the  $^1\text{H}$  NMR spectrum of the ternary complex. It can be observed that the signs of RVC are enlarged due to the degree of interaction with the liposomal vesicle. Figure 5B shows the control spectrum (out of resonance) and Figure 5A the STD spectrum. In the region of 3 to 4 ppm, the signals are more intense; they refer to the HP- $\beta$ CD hydrogens and PEG polymer (which coats the surface of the SL). Due to the overlap of signals, this region was discarded for STD analysis.

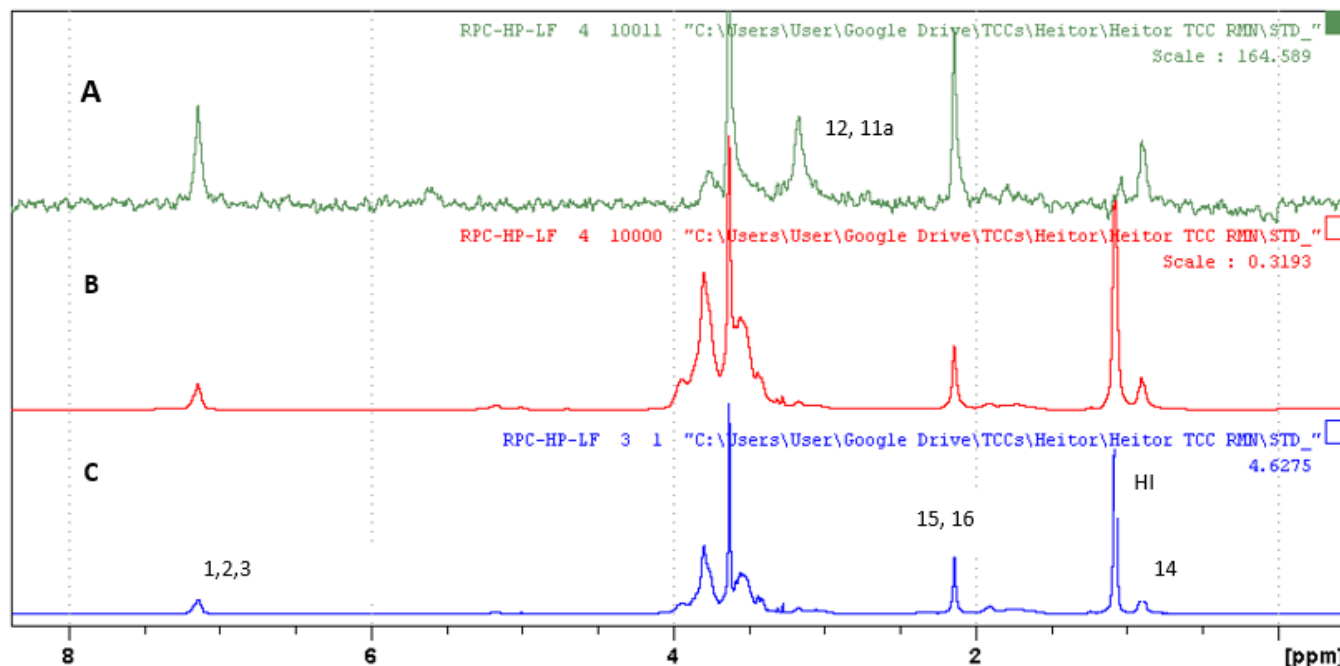


**Figure 5.** (A) STD spectrum (radiating at  $-0.5$  ppm); (B) control spectrum (radiating at  $30$  ppm); (C)  $^1\text{H}$  NMR spectrum (400 MHz,  $\text{D}_2\text{O}$ /residual  $\text{H}_2\text{O}$  reference at  $4.7$  ppm) of RVC/HP- $\beta$ CD/SL complex [ $50 \text{ mmol L}^{-1}$ ]. Total saturation time  $2.55$  s.

The RVC hydrogens with higher saturation transfer intensity were those of the aromatic ring 100% (H1, H2, H3), followed by H15–H16 and H14 34% and 35%, respectively. In the STD spectrum, H12 and H11a signals were also observed, but it was not possible to calculate the std transfer value because its intensity was not significant in the control spectrum. Thus, other signals show a greater intensity and overlap their maximum intensity. However, it can be considered that it has been complexed in the liposomal vesicle.

HP- $\beta$ CD hydrogens also showed saturation transfer. Hydrogens in the region between 3–4 ppm were not considered due to the overlap of signals. HI presented 0.4% in saturation transfer, indicating the lowest transfer value, as shown in Table 3.

The SL saturation transfer values for RVC and HP- $\beta$ CD hydrogens confirm the encapsulation of the RVC/HP- $\beta$ CD inclusion complex in SL vesicles. The STD spectrum shows that the aromatic part presents greater interaction with the liposomal vesicle since the Hs of the N-propyl amine and piperidine ring are also interacting with the SL, although with lower intensity.

For a better understanding of the complex interactions involving local anesthetics, the spectroscopic technique of  $^1\text{H}$  STD and DOSY has been applied, which shows suggestions of topologies and possible interactions among the molecules involved in the complex. Cabeça et al. [33] studied the mixture of prilocaine/ $\beta$ CD/EPC at different pHs and reported that prilocaine molecules were incorporated into liposomes. With the aid of the  $^1\text{H}$  STD technique, it was observed that prilocaine was released from  $\beta$ CD to liposome vesicles, and the formation of the PLC-Liposomes complex was higher at pH 10. Martins et al. [34] observed a strong interaction between the antibiotic dapson and egg phosphatidylcholine liposome (EPCL), with the complete insertion of dapson in the lipid bilayer of the liposome.



The authors reported that this type of system may be an alternative application for a low-soluble substance. In addition, embroidery may be useful for investigating other binary/ternary mixtures in solution.

### 2.3. Analysis of Particle Size and Zeta Potential

The analyses of particle size, polydispersity index (IP), and zeta potential (PZ) are shown in Table 4. Values of  $200 \pm 0.91$  nm and  $200 \pm 0.88$  nm for the binary complex of BTB/SL and RVC/SL and  $229 \pm 0.91$  nm and  $285 \pm 0.91$  nm for the ternary complex of BTB/HP- $\beta$ CD/SL and RVC/HP- $\beta$ CD/SL are indicated, respectively.

**Table 4.** Diameter of the vesicle liposome, polydispersity value and zeta potential.

Particles	Size (nm)	IP	PZ (mV)
SL	$202 \pm 1.02$	0.30	$-22.0 \pm 0.90$
BTB/SL	$200 \pm 0.91$	0.40	$-23.5 \pm 0.63$
BTB/HP- $\beta$ CD/SL	$229 \pm 0.91$	0.36	$-25.1 \pm 0.26$
RVC/SL	$200 \pm 0.88$	0.40	$-22.5 \pm 0.60$
RVC/HP- $\beta$ CD/SL	$285 \pm 0.91$	0.40	$-25.1 \pm 0.26$

SL—Stealth Liposome; BTB/SL—Butamben and Stealth Liposomes; BTB/SL/HP- $\beta$ CD:BTB—Stealth Liposomes, 2-Hydroxypropyl- $\beta$ -cyclodextrin and butamben; RVC/SL—Ropivacaine and Stealth Liposome; SL/HP- $\beta$ CD/RVC—Stealth liposomes, 2-Hydroxypropyl- $\beta$ -cyclodextrin and ropivacaine.

The results indicate that liposome vesicles were homogeneous even after the addition of BTB, RVC, and the HP- $\beta$ CD:RVC complex with polydispersity index with lower values  $\leq 0.4$ . This result points to a formulation close to homogeneity among SL, BTB, RVC, and HP- $\beta$ CD.

The surface load of vesicles for both ternary and binary complexes was negative and close ranging from 22 to 25 (Table 4). According to Cavalcanti et al., [25] IP ranges from 0 for homogeneous to 1 for polydispersed samples, since it is a measure of the amplitude of the size distribution, that resulted from the cumulative analysis of dynamic light dispersion (DLS) data. An IP equal to 1 indicates large variations in particle size, and a value close to 0 indicates a population of monodispersed particles (Lacatusu et al., [35]).

## 3. Materials and Methods

### 3.1. Materials

1,2-dipalmitoyl-sn-glycero-3-phosphocholine (DPPC); 1,2-distearoil-sn-glycero-3-phosphoethanolamina N[methoxy(polyethylene glycol)]-2000 (DSPE-PEG-2000); cholesterol were acquired from Avanti<sup>®</sup> polar lipids; Deuterated solvents; Ropivacaine (RVC) ((2S)-N-(2,6-Dimethylphenyl)-1-propyl-2-piperidinecarboxamide) and Butamben (BTB) Butyl 4-aminobenzoate, were acquired from Sigma Aldrich, São Paulo, SP, Brazil.

### 3.2. Preparation of the Complex between Local Anesthetics RVC or BTB in HP- $\beta$ CD

The inclusion complex BTB/HP- $\beta$ CD or RVC/HP- $\beta$ CD was prepared by mixing an equimolar amount of BTB and RVC in HP- $\beta$ CD (1:1) in sodium phosphate pH buffer solution 7.4. The mixture was left on a stirrer table for 24 h and then filtered in polycarbonate membrane (millex filter, MilliporeSigma, Burlington, MA, USA with 0.45  $\mu$ m pore).

### 3.3. RVC or BTB Calibration Curve

For the preparation of the calibration curve, BTB samples were prepared in phosphate pH buffer solution 7.4, varying the concentration from 0.014 to 0.066 mM. In order to obtain the RVC curve form, samples of RVC were prepared in phosphate-buffered solution pH 7.4 with concentration ranging from 0.1 to 0.54 mM. After that, the samples were taken to UV-vis.

### 3.4. Preparation of BTB Solutions for the Determination of Maximum Solubility ( $S_0$ ) in Sodium Phosphate Buffer pH 7.4

For the determination of the maximum solubility of BTB in sodium phosphate buffer pH 7.4, the methodology available in the Brazilian Pharmacopoeia 5th Edition (ANVISA, 2010) was used. The preparation of the solutions consisted of the addition of excess drug (BTB) (5, 10, 20, 30, 40, 50 mM) to constant volumes of solvent (3 mL), aiming at obtaining a saturated solution. According to the procedure systematized by Pharmacopoeia, the total content of solute in UV-vis solutions was determined.

### 3.5. Complexing Efficiency and Phase Solubility of the BTB/HP- $\beta$ CD and RVC/HP- $\beta$ CD

The complex formed between BTB and HP- $\beta$ CD was prepared in pH 7.4 buffer solution (sodium phosphate buffer 0.05 mM), varying the concentrations of HP- $\beta$ CD 0.001 to 0.5 mM, with an excess BTB (150 mM). The solutions were left on an agitator table for 24 h. The samples were filtered in polycarbonate membrane (millex filter, Millipore, USA with 0.45  $\mu$ m pore) and taken for UV-vis analysis. For the RVC and HP- $\beta$ CD complex, the variation in HP- $\beta$ CD concentration was 0.001 to 0.4 mM with excess RVC (70 mM). The mixture was stirred at room temperature for 24 h to achieve balance [25]. The sample was filtered in a membrane of 0.45 one (Millipore). The concentration of each LA for each sample was determined by UV spectrophotometry at 263 nm for RVC and 282 nm for BTB (Spectrometer Lambda 25). The association constant ( $K_a$ ) was determined from the slope of the linear relationship between the molar concentrations of LA in soluble medium versus the molar concentration of HP- $\beta$ CD according to Equation (5) [23]. The encapsulation efficiency (EE) of the LAs was determined from the data of the phase solubility curve and according to Equation (6) [22]. The drug/cyclodextrin ratio can be found in Equation (7) [7].

$$K = \frac{\text{slope}}{S_0 \times (1 - \text{slope})} \quad (5)$$

$$EE = \frac{\text{slope}}{1 - \text{slope}} \quad (6)$$

$$\text{LA} : \text{HP-}\beta\text{CD} = 1 : 1 + \frac{1}{EE} \quad (7)$$

where  $S_0$  is the aqueous solubility of LA in the absence of HP- $\beta$ CD.

### 3.6. Preparation and Encapsulation of LA in Long-Circulation Liposomes (RVC/SL and BTB/SL)

Liposomes were prepared using the lipid film method [36]. Stealth liposomes were formulated from egg phosphatidylcholine (EPC), cholesterol, and polyethylene glycol DSPE-PEG-2000 at a molar ratio of 54:41:5. Lipids were solubilized in chloroform containing 10 mM of RVC or BTB. The solvent was removed at room temperature to obtain a lipid film. Then, the lipids were hydrated with a pH 7.4 phosphate-buffered solution and stirred in the vortex. The complex was left in balance for 2 h. The formulation was then extruded 13 times in 400 nm polycarbonate membrane in an Avanti mini extruder.

### 3.7. Ternary Complex Preparation (RVC/HP- $\beta$ CD/SL)-(BTB/HP- $\beta$ CD/SL)

The stealth liposomes were prepared from the compounds of egg phosphatidylcholine (EPC), cholesterol (Sigma Aldrich, São Paulo, SP, Brazil), and DSPE-PEG-2000 (Avast lipids) at a molar ratio of 54:41:5. The components were solubilized in chloroform and left at room temperature to obtain a lipid film [37]. Then, the lipid film was hydrated with the binary complex of (RVC/HP- $\beta$ CD) or (BTB/HP- $\beta$ CD), taken to the vortex, and left in equilibrium for 2 h. The liposomal suspension formed multilamellares liposomes, which in turn were extruded into a 400 nm polycarbonate membrane in an Avanti mini extruder to obtain small unilamellares vesicles (SUV).

### 3.8. Determination of Encapsulation Efficiency of the LA/SL and LA/HP- $\beta$ CD/SL Complex (SL = RVC or BTB)

The efficiency of LA encapsulated in liposomes was determined using the ultrafiltration/ultracentrifugation technique (Millipore, USA, ME Cut-off 10,000Da) [28]. A sample amount of 400  $\mu$ L containing the LA/SL or LA/HP- $\beta$ CD/SL complex was placed in a filter unit and subjected to ultracentrifugation (13,000 rpm for one hour). A quantity of 100  $\mu$ L that passed through the filter (free LA) was diluted in 3 mL of phosphate buffer (pH 7.4) and quantified using UV spectrophotometry at 263 nm for RVC 282 nm for BTB. The efficiency calculation was performed using Equation (8) [28].

$$EE\% = \frac{[LA]_{total} - [LA]_{diffused.AL}}{[LA]_{total}} \times 100 \quad (8)$$

### 3.9. Nuclear Magnetic Resonance

NMR experiments were carried out at the Laboratory of Nuclear Magnetic Resonance of the State University of Londrina—UEL. The equipment used was the Bruker 400 MHz for hydrogen frequency (Bruker Corporation, Billerica, MA, USA), carried out with “software” Bruker standards under typical conditions. The experiments were conducted at 25 °C, applying as reference the peak of the residual deuterium (4.70 ppm), which was used as field lock and adjusted the homogeneity of the magnetic field.

DOSY design: For all experiments, 16 different gradient amplitudes were used with diffusion time optimization of 0.06 s. The DOSY Toolbox [36] data processing program was employed. The coefficients calculated for each selected signal were listed together with the respective standard deviations. The value of the diffusion coefficient and standard deviation of each species involved in the analysis was given through the arithmetic mean of all coefficients of the same species. Coefficients with values different from those presented by the majority were discarded. The results of the DOSY analysis method are two-dimensional spectra with  $^1\text{H}$  NMR chemical displacements on one axis and the calculated diffusion coefficient ( $\text{m}^2\text{s}^{-1} \times 10^{-10}$ ) in another dimension. The mean time of acquisition of the experiment was 25 min. The complex diffusion coefficient is determined based on the exchange between a free and complex state of the ligand. The complexed molar fraction ( $f_x$ ) and association constant ( $K_a$ ) can be calculated using Equations (9) and (10), respectively [23].

$$f_x = \frac{(D_{free} - D_{complex})}{(D_{free} - D_{host})} \quad (9)$$

$$K_a = \frac{f_x}{((1 - f_x)([host] - f_x [guest]))} \quad (10)$$

STD experiment: The STD experiments were selectively saturated using Gaussian pulse trains at  $-0.5$  ppm for resonance acquisition and 30 ppm for out-of-resonance acquisition. The experiments were processed using the TOP SPIN program. Saturation time was 2.55 s.

### 3.10. Determination of Size, Zeta Potential and SL Particle Polydispersivity Index

The average particle size, as well as zeta potential and liposome polydispersivity index were determined through dynamic light scattering experiments carried out at the Biology Institute of Unicamp. The determination was performed by an average of the data obtained in the experiments. The device used in the study was a Zeta Size particle analyzer from Malvern Instruments (Worcestershire, UK).

## 4. Conclusions

The molecular interactions of local anesthetics BTB and RVC with HP- $\beta$ CD were identified by the DOSY technique and also by the  $^1\text{H}$  chemical shift, which the aromatic rings of the drugs interacted with the HP- $\beta$ CD cavity. It was observed in the normalized  $^1\text{H}$ -STD that

the BTB/HP- $\beta$ CD complex showed variations in intensity of all  $^1\text{H}$  signals, with aromatics hydrogens showing the highest intensity values. HP- $\beta$ CD  $^1\text{H}$  signals in the region between 3 and 4 ppm were also observed. This result can confirm the encapsulation of the binary complex in the liposomal vesicle. For the RVC anesthetic, lower values of encapsulation were observed both in the binary complex and in the liposomes (DOSY). The complex RVC/HP- $\beta$ CD showed an alternative of topology whit the aromatic hydrogens and the piperidine ring in hydrophobic cavity of HP- $\beta$ CD. For the  $^1\text{H}$ -STD of RVC/HP- $\beta$ CD complex, the RVC hydrogens with higher saturation transfer intensity were those of the aromatic ring, and there are HP- $\beta$ CD  $^1\text{H}$  signals in the region between 3 and 4 ppm too. In general, these results are promising, indicating that  $^1\text{H}$  NMR techniques for mapping the bonds intermolecular of complexes may be utilized. This opens the door to further studies, aiming at better systems for drug protection and release, since the field of study in supramolecular chemistry grows exponentially.

**Author Contributions:** Conceptualization, G.K.S. and L.F.C.; methodology, A.G., H.R.N. and L.F.C.; software, L.F.C.; validation, A.J.M. and E.d.P.; formal analysis, L.F.C.; investigation, A.G., H.R.N. and L.H.N.; resources, G.K.S. and L.F.C.; data curation, A.G., H.R.N. and L.F.C.; writing—original draft preparation, G.K.S. and L.F.C.; writing—review and editing, G.K.S. and L.F.C. All authors have read and agreed to the published version of the manuscript.

**Funding:** This research was funded by MCTI/CNPq 14/2014, process number 448908/2014-0.

**Institutional Review Board Statement:** Not applicable for studies not involving humans or animals.

**Informed Consent Statement:** Not applicable.

**Data Availability Statement:** Not applicable.

**Acknowledgments:** The authors are thankful to CAPES (Coordination for the Improvement of Higher Education Personnel), CNPq (National Counsel of Technological and Scientific Development, (Process n $^\circ$  448908/2014-0); (Gredson Keiff Souza, Process n $^\circ$  150270/2021-6); (Anita Jocelyne Marsaiolo Process n $^\circ$  307885/2013-5; FAPESP-Research Support Foundation of the State of São Paulo, 2018/07078-0), and to the Laboratory of Nuclear Magnetic Resonance, State University of Londrina (UEL) for the support in the analysis.

**Conflicts of Interest:** The authors declare no conflict of interest.

**Sample Availability:** Samples of the compounds are available from the authors.

## References

1. Pastor, A.; Martínez-Viviente, E. NMR spectroscopy in coordination supramolecular chemistry: A unique and powerful methodology. *Coord. Chem. Rev.* **2008**, *252*, 2314–2345. [[CrossRef](#)]
2. Kupče, Ě.; Frydman, L.; Webb, A.G.; Yong, J.R.J.; Claridge, T.D.W. Parallel nuclear magnetic resonance spectroscopy. *Nat. Rev. Methods Primers* **2021**, *1*, 27. [[CrossRef](#)]
3. Periasamy, R. Cyclodextrin-based molecules as hosts in the formation of supramolecular complexes and their practical applications—A review. *J. Carbohydr. Chem.* **2021**, *40*, 135–155. [[CrossRef](#)]
4. Mo, H.P.; Pochapsky, T.C. Intermolecular interactions characterized by nuclear overhauser effects. *Prog. Nucl. Magn. Reson. Spectrosc.* **1997**, *30*, 1–38. [[CrossRef](#)]
5. Morris, K.F.; Johnson, C.S. diffusion-ordered 2-dimensional nuclear-magnetic-resonance spectroscopy. *J. Am. Chem. Soc.* **1992**, *114*, 3139–3141. [[CrossRef](#)]
6. Meyer, B.; Peters, T. NMR Spectroscopy techniques for screening and identifying ligand binding to protein receptors. *Angew. Chem. Int. Ed.* **2003**, *42*, 864–890. [[CrossRef](#)]
7. Jambhekar, S.S.; Breen, P. Cyclodextrins in pharmaceutical formulations II: Solubilization, binding constant, and complexation efficiency. *Drug Discov. Today* **2016**, *21*, 363–368. [[CrossRef](#)]
8. Szente, L.; Singhal, A.; Domokos, A.; Song, B. Cyclodextrins: Assessing the impact of cavity size, occupancy, and substitutions on cytotoxicity and cholesterol homeostasis. *Molecules* **2018**, *23*, 1228. [[CrossRef](#)]
9. Venturini, C.G.; Nicolini, J.; Machado, C.; Machado, V.G. Propriedades e aplicações recentes das ciclodextrinas. *Quim. Nova* **2008**, *31*, 360–368. [[CrossRef](#)]
10. Freitas, C.F.; Calori, I.R.; Tessaro, A.L.; Caetano, W.; Hioka, N. Rapid formation of small unilamellar vesicles (SUV) through low-frequency sonication: An innovative approach. *Colloids Surf. B* **2019**, *181*, 837–844. [[CrossRef](#)]
11. Vieira, A.L.N.; Franz-Montan, M.; Cabeça, L.F.; Paula, E. Anaesthetic benefits of a ternary drug delivery system (Ropivacaine-in-Cyclodextrin-in-Liposomes): In-Vitro and in-vivo evaluation. *J. Pharm. Pharmacol.* **2020**, *72*, 396–408. [[CrossRef](#)] [[PubMed](#)]

12. Maritim, S.; Boulas, P.; Lin, Y. Comprehensive analysis of liposome formulation parameters and their influence on encapsulation, stability and drug release in glibenclamide liposomes. *Int. J. Pharm.* **2021**, *592*, 120051. [CrossRef] [PubMed]
13. Holzschuh, S.; Kaeß, K.; Fahr, A.; Decker, C. Quantitative In vitro assessment of liposome stability and drug transfer employing asymmetrical flow field-flow fractionation (AF4). *Pharm. Res.* **2016**, *33*, 842–855. [CrossRef] [PubMed]
14. Nag, O.K.; Awasthi, V. Surface engineering of liposomes for stealth behavior. *Pharmaceutic* **2013**, *5*, 542–569. [CrossRef] [PubMed]
15. Batista, C.M.; Carvalho, C.M.B.; Magalhães, N.S.S. Lipossomas e suas aplicações terapêuticas: Estado da arte. *Rev. Bras. Ciênc. Farm.* **2007**, *43*, 167–179. [CrossRef]
16. Immordino, M.L.; Dosio, F.; Cattel, L. Stealth liposomes: Review of the basic science, rationale, and clinical applications, existing and potential. *Int. J. Nanomed.* **2006**, *1*, 297–315.
17. Mowat, J.J.; Mok, M.J.; Macleod, B.A.; Madden, T.D. Liposomal bupivacaine—Extended duration nerve blockade using large unilamellar vesicles that exhibit a proton gradient. *Anesthesiology* **1996**, *85*, 635–643. [CrossRef]
18. Franz-Montan, M.; Silva, A.L.R.; Cogo, K.; Bergamaschi, C.C.; Volpato, M.C.; Ranali, J.; Paula, E.; Groppo, F.C. Liposome-encapsulated ropivacaine for topical anesthesia of human oral mucosa. *Anesth. Analg.* **2007**, *104*, 1528–1531. [CrossRef]
19. Franz-Montan, M.; De Paula, E.; Groppo, F.C.; Ranali, J.; Volpato, M.C. Efficacy of liposome-encapsulated 0.5% ropivacaine in maxillary dental anaesthesia. *Br. J. Oral.* **2012**, *55*, 454–458. [CrossRef]
20. Richard, B.M.; Ott, L.R.; Haan, D.; Brubaker, A.N.; Cole, P.I.; Nelson, K.G.; Ross, P.E.; Rebelatto, M.C.; Newton, P.E. The safety and tolerability evaluation of DepoFoam bupivacaine (bupivacaine extended-release liposome injection) administered by incision wound infiltration in rabbits and dogs. *Expert Opin. Investig. Drugs* **2011**, *20*, 1327–1341. [CrossRef]
21. Mura, P.; Maestrelli, F.; Gonzalez-Rodriguez, M.; Michelacci, I.; Ghelardini, C.; Rabasco, A. Development, characterization and in vivo evaluation of benzocaine-loaded liposomes. *Eur. J. Pharm. Biopharm.* **2007**, *67*, 86–95. [CrossRef] [PubMed]
22. Bezamat, J.M.; Yokaichiya, F.; Franco, M.K.K.D.; Castro, S.R.; Paula, E.; Cabeça, L.F. Complexation of the local anesthetic pramoxine with hydroxypropyl-beta-cyclodextrin can improve its bioavailability. *J. Drug Deliv. Sci. Technol.* **2020**, *55*, 101475. [CrossRef]
23. Higuchi, T.; Connors, K.A. Phase solubility techniques. *Anal. Chem. Instrum.* **1965**, *4*, 117–212.
24. Araujo, D.R.; Paula, E.; Fraceto, L.F. Anestésicos locais: Interação com membranas biológicas e com o canal de sódio voltagem-dependente. *Quím. Nova* **2008**, *31*, 1775–1783. [CrossRef]
25. Cavalcanti, I.M.F.; Mendonça, E.A.M.; Lira, M.C.B.; Honrato, S.B.; Camara, C.A.; Amorim, R.V.S.; Filho, J.M.; Rabello, M.M.; Hernandez, M.Z.; Ayala, A.P.; et al. The encapsulation of  $\beta$ -lapachone in 2-hydroxypropyl- $\beta$ -cyclodextrin inclusion complex into liposomes: A physicochemical evaluation and molecular modeling approach. *Eur. J. Pharm. Sci.* **2011**, *44*, 332–340. [CrossRef] [PubMed]
26. Barbosa, J.A.A.; Zoppi, A.; Quevedo, M.A.; Melo, P.N.; Medeiros, A.S.A.; Streck, L.; Oliveira, A.R.; Fernandes-Pedrosa, M.; Longhi, M.R.; Silva-Júnior, A.A. Triethanolamine stabilization of methotrexate- $\beta$ -cyclodextrin interactions in ternary complexes. *Int. J. Mol. Sci.* **2014**, *15*, 17077–17099. [CrossRef]
27. Moraes, C.M.; Abrami, P.; Gonçalves, M.M.; Filho, N.A.; Fernandes, S.A.; Paula, E.; Fraceto, L.F. Preparação e caracterização físico-química de complexos de inclusão entre anestésicos locais e hidroxipropil- $\beta$ -ciclodextrina. *Quím. Nova* **2007**, *30*, 777–784. [CrossRef]
28. Maestrelli, F.; González-Rodríguez, M.L.; Rabasco, A.M.; Ghelardini, C.; Mura, P. New “drug-in cyclodextrin-in deformable liposomes” formulations to improve the therapeutic efficacy of local anaesthetics. *Int. J. Pharm.* **2010**, *395*, 222–231. [CrossRef]
29. De Paula, E.; Cereda, C.M.S.; Tofoli, G.R.; Franz-Montan, M.; Fraceto, L.F.; Araújo, D.R. Drug delivery systems for local anesthetics, recent pat. *Drug Deliv. Formul.* **2010**, *4*, 23–34. [CrossRef]
30. Dehaghani, M.Z.; Bagheri, B.; Yousefi, F.; Nasiriasayesh, A.; Mashhadzadeh, A.H.; Zarrintaj, P.; Rabiee, N.; Bagherzadeh, M.; Fierro, V.; Celzard, A.; et al. Boron nitride nanotube as an antimicrobial peptide carrier: A theoretical insight. *Int. J. Nanomed.* **2021**, *16*, 1837–1847. [CrossRef]
31. Lin, S.Y.; Kao, Y.H. Solid particles of drug-beta-CD inclusion complexes directly prepared by a spray-drying technique. *Int. J. Pharm.* **1989**, *56*, 249–259.
32. Cabeça, L.F.; Fernandes, S.A.; Paula, E.; Marsaioli, A.J. Topology of a ternary complex (proparacaine- $\beta$ -cyclodextrin-liposome) by STD NMR. *Magn. Res. Chem.* **2008**, *46*, 832–837. [CrossRef] [PubMed]
33. Cabeça, L.F.; Figueiredo, I.M.; Paula, E.; Marsaioli, A.J. Prilocaine-cyclodextrin-liposome: Effect of pH variations on the encapsulation and topology of a ternary complex using  $^1\text{H}$  NMR. *Magn. Reson. Chem.* **2011**, *49*, 295–300. [CrossRef] [PubMed]
34. Martins, L.; Arrais, M.; Souza, A.; Marsaioli, A.  $^1\text{H}$  NMR studies of binary and ternary dapsone supramolecular complexes with different drug carriers: EPC liposome, SBE- $\beta$ -CD and  $\beta$ -CD. *Magn. Reson. Chem.* **2014**, *52*, 665–672. [CrossRef] [PubMed]
35. Lacatusu, I.; Badea, B.; Stan, R.; Meghea, A. Novel bio-active lipid nanocarriers for the stabilization and sustained release of sitosterol. *Nanotechnology* **2012**, *23*, 455702. [CrossRef]
36. DOSY Toolbox, Manchester NMR Methodology Group. Available online: <https://nmr.chemistry.manchester.ac.uk/?q=node/8> (accessed on 22 June 2022).
37. Haeri, A.; Sadeghian, S.; Rabbani, S.; Anvari, M.S.; Lavasanifar, A.; Amini, M.; Simin, D. Sirolimus-loaded stealth colloidal systems attenuate neointimal hyperplasia after balloon injury: A comparison of phospholipid micelles and liposomes. *S. Int. J. Pharm.* **2013**, *455*, 320–330. [CrossRef] [PubMed]